

# Modeling the impact of asteroids over Mexican territory

R. Gutiérrez-Zalapa

*Posgrado en Ciencias de la Tierra, Escuela Nacional de Estudios Superiores Morelia,  
Universidad Nacional Autónoma de México, Antigua Carretera a Pátzcuaro 8701, Morelia Michoacan México.*

M. Rodríguez-Martínez

*Escuela Nacional de Estudios Superiores Morelia, Universidad Nacional Autónoma de México,  
Antigua Carretera a Pátzcuaro 8701, Morelia Michoacan México.*

E. Aguilar-Rodríguez

*Instituto de Geofísica Unidad Michoacán, Universidad Nacional Autónoma de México,  
Antigua Carretera a Pátzcuaro, 8701, Morelia Michoacan México.*

J. Estevez-Delgado

*Facultad de Ciencias Físico-Matemáticas, Universidad Michoacana de San Nicolás de Hidalgo,  
Avenida F. J. Múgica, 58030, Morelia Michoacan México.*

Received 29 June 2023; accepted 14 September 2023

This work focuses on knowing the physical, environmental and population effects from the impact of an asteroid occurring in the Mexican territory. The work consists of the adaptation of routines product of previous works in the literature to generate a numerical code written in PyThon that allowed modeling this kind of phenomenon. Firstly, a map of the superficial densities of the Mexican territory has been developed with a resolution of  $0.5^\circ$  of longitude by  $0.5^\circ$  of latitude of the Earth. The map allows us to find the value of surface density in a specific geological area of the country. Once the surface density value was obtained, it is established as the value of the impact site (target). The model requires using fixed parameters, such as the diameter of the body, its density or mass, the angle of incidence and the density value at the impact site. The output, provides the impact velocity, as well as the energy released, diameter and depth of the crater, the magnitude of the earthquake as well as the damage on the surface. We studied the Chicxulub asteroid event in two hypothetical scenarios. Firstly, the atmospheric density profile was modified, allowing the calculation of a new value for the impact velocity. Secondly, we assume that the object hits with a fraction of the initial mass, and with this the impact velocity and its effects were recalculated for three different targets. They were used to calculate the infrastructure damage they would cause if the impact could occur today. Finally, the results obtained by our model were compared with the literature, showing that they are consistent with the observational data. Models such as this one contribute to having tools for the attention towards the prevention of this kind of event that in the context of the study risks from the space are necessary in Mexico.

*Keywords:* Asteroids impact; Chicxulub impact event; numerical model for asteroids' impacts; environmental and infrastructural damage by asteroids' impacts.

DOI: <https://doi.org/10.31349/RevMexFis.70.010701>

## 1. Introduction

There are several theories that try to explain the solar system formation. One of the most acceptable so far proposes that the formation and evolution of the solar system began 4,500 million years ago with the gravitational collapse of a small part of a giant molecular cloud [1]. Most of the collapsing material clumped together in the center, forming a proto-Sun, while the rest flattened into a protoplanetary disk from which the planets were formed [2]. The bodies that could not form a planet as simply trapped wandering bodies because of gravitational interaction in orbits around the Sun. These bodies were called asteroids or comets, and many of these collided with the Earth when it was forming; see for instance [3]. The attention of this work is focused on this class of wandering body, in particular Near Earth Objects (NEO), which trace an orbit close to the Earth. In other words, because of the implications of their proximity or possible collision, is con-

sidered to have generated substantial changes in the history of the planet, such as in the configuration of geological and biological history [4].

Modeling the impact of asteroids on a specific territory, such as Mexican territory, involves various factors and considerations. It is well known that there are several studies related to the impact of an NEO on the Earth's surface. For example, [5] used a hydrocode to estimate the impact effects of a rocky, non-variable-mass NEO. On the other hand, [6] employed an equation that describes the change in mass at the impact of porous bodies. There is also work on the morphology of craters formed by debris pile objects or binary objects [7, 8], respectively. In relation to the latter, there are laboratory simulations that recreate the impacts of NEOs on the Earth's surface, using various materials that act as impactors and as targets, to obtain results on the size of the craters [9, 10]. Additionally, there are also works that are

related to the impact of bodies in the ocean [11] and its repercussions in coastal areas, as well as the magnitude of the earthquake (measured on the Richter scale) that this impact would cause.

In this work we present a numerical model for the impact of an NEO in Mexican territory, based firstly on the calculations made by [12] but to which the following equations have been added: one equation to calculate the impact velocity, which is a modification of the one proposed by [13]; and another to calculate the final mass based on the initial mass, composition and the morphology of the object [14–16]. Our model uses this equation when the value of the density of the body is unknown. We also added another equation to calculate the magnitude of the earthquake caused by the impact and finally one equation to calculate the area affected by overpressure, as well as a routine that allows calculating the percentage of the environment seriously affected. In this context, we have specifically focused on asteroid characterization, blast and crater formation and finally the damage assessment, adapted from [12].

This article is presented as follows: in Sec. 2, we describe the mathematical model on which our work is based, containing all the components necessary for describing the possible behaviour in the Mexican territory. In Sec. 3 we describe the environmental effects of body impact, focusing on the damaged population and the area affected by overpressure. Section 4 introduces the case study of the Chicxulub event, in which we show the behavior of the impact parameters such as velocity, the energy released, diameter and depth of the crater as well as the magnitude of the earthquake. In addition, we recreate the Chicxulub event for three different target values and a mass loss factor. With these data and information from the website [17], we present the possible infrastructural damage (in three different geographical sites) that the impact would generate. Finally, in Sec. 5, we discuss our results.

## 2. Model

The impact of an asteroid on the Earth surface requires specifically focusing on the asteroid characterization, blast and crater formation and the damage assessment, among other variables. It is important to mention that mathematical modeling has been developed for its application in the Mexican territory, taking into account elements of the work of [12], and others that allowed obtaining the equations that describe the impact energy,  $E_i$ , the diameter and depth of the crater,  $D_{tc}$  and  $d_{tc}$ , respectively, and the radius of the fireball,  $R_f$ . In the following sections, we will present the additional components of this model.

### 2.1. Terminal velocity

Parameters such as the impact velocity are necessary to quantify the spatial scales when an asteroid collides with the Earth's surface. In our model, we have used the kinetic energy equation provided by [13, 18] which we modified by tak-

ing into account an atmospheric density profile for a height  $h = 0$ . This modification is consistent with that proposed by [19], which establishes that for spherical objects that impact the Earth's surface, the terminal velocity of the body with respect to its initial velocity is between  $2/3$  to  $4/5$  times, while considering a mass loss of between 30% to 60% due to ablation process due the pass through the atmosphere. In this context, the terminal velocity can be obtained as follows:

$$V_i = \sqrt{\frac{4\rho_i dg}{3C_d \rho_a(h)_{h=0}}}, \quad (1)$$

where  $\rho_i$  and  $d$  are the density and diameter of the meteoroid, respectively,  $g$  is the gravitational acceleration constant,  $C_d = 0.5$  is the drag coefficient [13] and  $\rho_a(h)_{h=0}$  is the atmospheric density evaluated on the ground. The mathematical expression suitable for Eq. (1) has to be like  $\rho_a(h) = \alpha e^{\delta_1 h} + \beta e^{\delta_2 h}$ , with  $\alpha + \beta > 0$  and  $\delta_1, \delta_2 \in R$ . A similar deduction for the Eq. (1), which does not contemplate an atmospheric density profile, is shown in Ref. [20].

### 2.2. Intensity of earthquake

Our model considers a module to evaluate the fraction of kinetic energy transformed into seismic wave energy, if an impact were to occur. This module calculates the magnitude of the earthquake; the value of this fraction ranges from  $10^{-5} - 10^{-3}$  [21]. In the energy-magnitude relationship for an earthquake, [22] used it to calculate the intensity of the earthquake but with the Richter scale.

In 2012, the International Seismological Association decided to no longer use the Richter scale to measure earthquakes because it is not longer representative of the energy that is released by an earthquake or the intensity of earthquakes. In this context, we decided to use the calculations made by [23], which are the basis of our model by adding the new scale, in comparison with [12]. In this way, in our model the magnitude of an earthquake is related to the energy radiated,  $E$  in Joules ( $J$ ) [24] as:

$$HK_s = \frac{\log_{10}(2 \times 10^4 E_i) - 9.05}{1.5}. \quad (2)$$

Furthermore, [25] used the concept of seismic energy flux density defined as  $10^{-5}$  times the total kinetic energy,  $E_{ac}$  to calculate the seismic effects caused by the shock wave produced by the rupture of a meteoroid.

### 2.3. Geological composition

One of the main considerations that we took into account to represent the physical phenomena related to the impact of an object over the entire Mexican territory was to know the geological composition at a deep of 10 m. To resolve this, we generate a matrix of density values using the GeoMapApp software [26], which software helps us to know the surface

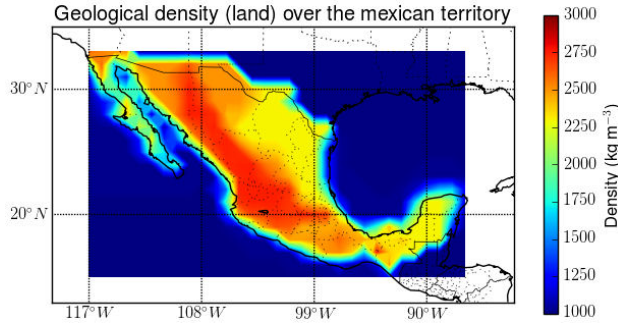


FIGURE 1. Map of the surface density of the Mexican territory. This map has a resolution of  $0.5^\circ$  longitude per  $0.5^\circ$  latitude per 10 m in deep.

density of the territory well by generating a matrix of values over the entire Mexican territory. The grid was divided into subregions of  $0.5^\circ$  of latitude by  $0.5^\circ$  of longitude. The density matrix ( $0.5^\circ \times 0.5^\circ \times 10$  m on average) was stored in a file that is read by the model developed in the Python programming language. Generally, this allows us to represent in a map of the Mexican region the surface density of the entire country (see Fig. 1).

It is important to mention that there are several works related to modeling the density of the Earth as a function of its radius, suggesting that for the first 100 km of depth, the average density remains constant with respect to the density on the surface [27]. In order to analyze the impact of asteroids larger than 0.54 m and reproduce their effects well, we consider that the target density uses this approximation.

### 3. Environment effects

Another property of interest is the environmental damage caused by the impact of an NEO in the Mexican territory. The studies and data from [28] related to the estimation of the severely affected world population with respect to the energy released, see Figure in the upper panel 2. Using these data and a model based on B-Splines and Vandermonde matrices, the function that relates the energy released to the affected population was obtained. We used B-Splines to determine the polynomial expression that relates environmental damage as a function of the energy released, allowing us to use the smallest number of degrees of freedom, while the use of Vandermonde matrices served to interpolate the polynomial that was fitted to the aforementioned data. In particular, it was possible to determine the energy necessary to significantly damage the total world population, which is approximately  $1.2 \times 10^{24}$  J. In the same way, the energy released by the impact of the Chicxulub asteroid is in the order of  $\sim 10^{23}$  J needed to affect 90% of the environment of Earth. This value is reached with the aforementioned impact energy  $E_i$ , a value consistent with [12, 29].

### 3.1. Surface and infrastructure affected

To know the surface reached ( $S_R$ ) that would be damaged by the impact of an asteroid, we use the analysis made by [30], which studies the affected surface (by release of energy) at a pressure of at least 4 PSI or  $\approx 27579$  Pa. With this analysis, we can establish the area of damage in those places enclosed by the radius  $R$  where the pressure is exceeded by 27579 Pa, which represents the pressure can break windows as well as crush cars. The mathematical expression in this case is a function of the height  $h$  in kilometers at which the energy release occurs, where the energy  $E$  is in units of megatons:

$$R = 2.1h - 0.5h^2E^{-1/3} + 5.1E^{1/3}. \quad (3)$$

In our work, we have considered that the impact occurs at a height  $h = 0$ . With this assumption by using the work of [31] to know the total area that would be damaged from the impact, we modified the Eq. (3) as

$$S_R = 25.8\pi E^{2/3}. \quad (4)$$

### 4. Case study analysis

In order to test the model, we applied this to the Chicxulub event that occurred 65 million years ago according to [32–34]. To recreate the Chicxulub asteroid impact scenario, we use the next parameters of the literature:  $d_i = 11500$  m,  $\rho_i = 2750$  kg/m<sup>3</sup>,  $\theta_0 = 45^\circ$  and  $v_i = 17$  km/s, which are nominal values are from [35].

From our model, we obtained the following results: in Fig. 2 the lower panel shows the curve that describes the behavior of the impact energy as a function of velocity. In particular, it is observed that given an impact velocity of

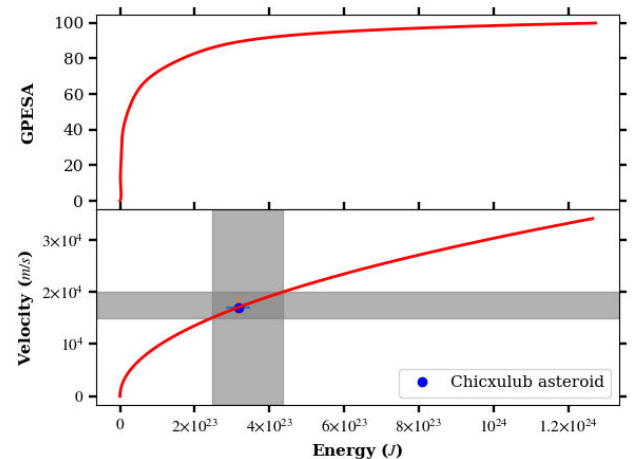


FIGURE 2. Upper panel shows the behavior of the Global Percentage of the Environment Seriously Affected (GPESA) as a function of energy released. For a damage of 100% an energy of the order  $\sim 1 \times 10^{24}$  J is required. The lower panel shows the behavior of the energy as a function of the impact velocity. For  $v_i = 17$  km/s, the  $\cdot$  indicates the value obtained for  $E_i = 3.2 \times 10^{23}$  J value that matches [36, 37].

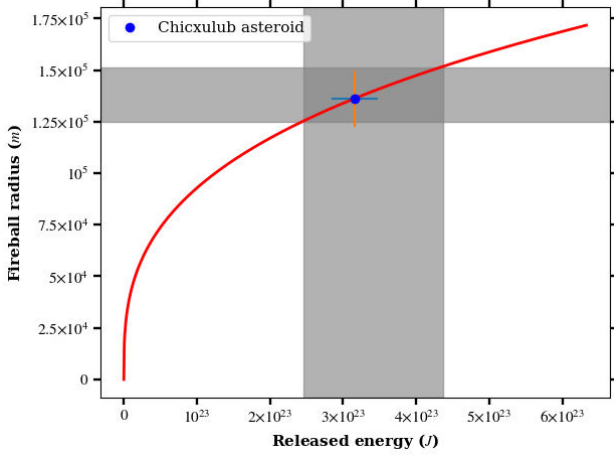


FIGURE 3. This plot shows the curve of the radius of the fireball as a function of the energy released. The  $\cdot$  indicates the value obtained for  $R_f = 1.3 \times 10^5$  m.

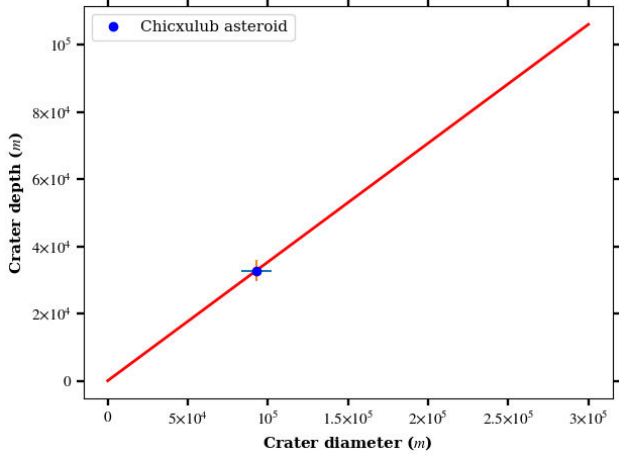


FIGURE 5. Graphical analysis of the depth of the crater as a function of the crater diameter. The  $\cdot$  indicates the value for the depth  $d_{tc} = 4.8 \times 10^4$  m.

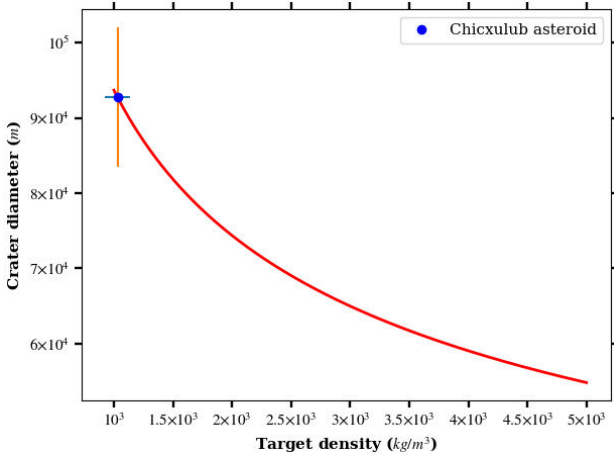


FIGURE 4. Graphical analysis of the diameter of the crater as a function of the density of the target as a function of its diameter. The  $\cdot$  indicates the value of the diameter of the crater obtained  $D_{tc} = 1.3 \times 10^5$  m.

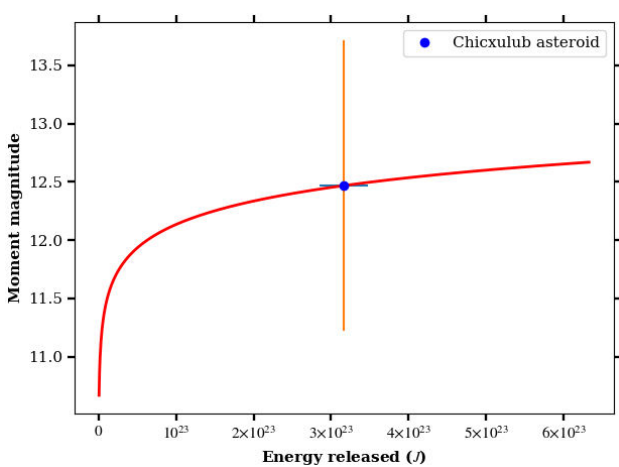


FIGURE 6. Graphical analysis of the earthquake as a function of the energy by Chicxulub asteroid. The  $\cdot$  indicates the value obtained for the magnitude of the earthquake  $M_w = 12.4$ .

$v_i = 17$  km/s, the energy released would be  $E_i = 3.2 \times 10^{23}$  J. The horizontal gray band corresponds to the minimum and maximum values of impact velocity [38, 39]. The vertical gray band corresponds to the minimum and maximum energy values corresponding to the aforementioned impact velocities.

Figure 3 shows the behavior of the fireball radius as a function of the released energy. It can be seen that the size of the fireball radius would be  $f_R = 1.5 \times 10^5$  m, which are data in the order of magnitude proposed by [40, 41]. The vertical band corresponds to the minimum and maximum values of energy released. Similarly, the horizontal gray band indicates the minimum and maximum radius of the fireball in relation to the aforementioned released energies.

Figure 4 describes the behavior of the crater diameter caused by the impact, as a function of the target density. Specifically, it is indicated that for a target density of  $\rho_t = 1030$  kg/m<sup>3</sup> (a value close to the moment of impact [40]),

the diameter would be  $D_c = 9.3 \times 10^4$  m. Figure 5 describes the curve of the depth of the crater as a function of its aforementioned diameter, obtaining that the depth would be  $d_{tc} = 2.6 \times 10^4$  m. Our values are consistent with that reported by [42].

Figure 6 shows the earthquake magnitude curve as a function of energy, in which it is inferred that the magnitude of the earthquake would be  $M_w = 12.4$ , to put this value in context, the largest recorded earthquake was that of Valdivia Chile in 1960 with a value of  $M_w = 9.6$  [23]. This value is in the order of magnitude with that indicated by [37]. Figure 7 shows the area that is affected by overpressure as a function of the radiated energy. The affected area would be  $S_R = 1.49 \times 10^7$  km<sup>2</sup>. In all previous graphs, an error bar of 10% has been added to the result obtained.

To contextualize the relevance of the atmospheric density profile in the impact velocity calculation, the Chicxulub event was recreated using the [43] profile. From the data in Table I,

TABLE I. Results obtained implementing two density profiles.

Parameter/Atmospheric density profile	[12]	[43]	Variation
Impact velocity (m/s)	$2 \times 10^4$	$1.8 \times 10^4$	10%
Energy released (J)	$4.5 \times 10^{23}$	$4.1 \times 10^{23}$	8.8%
Fireball radius (m)	$1.5 \times 10^5$	$1.4 \times 10^5$	< 1%
Diameter crater (m)	$1.4 \times 10^5$	$1.3 \times 10^5$	< 1%
Depth crater (m)	$4.9 \times 10^4$	$4.8 \times 10^4$	< 1%
Earthquake magnitude	12.6	12.5	< 1%
Area affected by overpressure ( $\text{km}^2$ )	$1.8 \times 10^7$	$1.7 \times 10^7$	< 1%

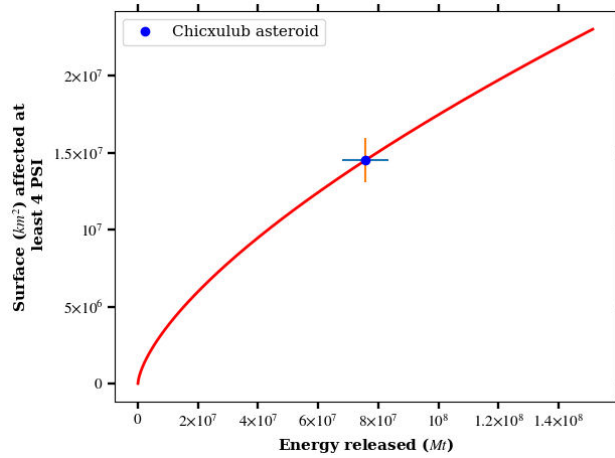


FIGURE 7. Graphical analysis of the surface affected by overpressure as a function of the energy by Chicxulub asteroid. The  $\cdot$  indicates the value obtained for the area affected by overpressure  $S_R = 1.4 \times 10^7 \text{ km}^2$ .

it can be deduced that by using the atmospheric density profile of [43] in our model, we obtain values that better fit what was proposed by [12, 34]. In this order, the value of the impact velocity differs by one-tenth, and the energy released and the radius of the fireball are in the same order of magnitude. The dimensions of the crater differ by one hundredth, while the magnitude of the earthquake does so by one-tenth. Finally, the area affected by overpressure is in the same order of magnitude.

The methodology used to obtain the damage to the infrastructure, related to the impact of the body, consisted of using the [17] website, specifically the *information polygons* tool, which yields results of the number of dwellings in a region well defined by the user. We delimit this region using the values of the diameter of the crater and the radius of the fireball. Based on the above, we can infer the possible infrastructural damage that the impact of the Chicxulub object could currently cause. For this we have defined three hypothetical targets; the first will be the place where the Chicxulub object originally collided,  $\rho_t = 1030 \text{ kg/m}^3$ . To define the second and third targets, we used the map in Fig. ???. We define the second target at the coordinates  $25^\circ\text{N}$ ,  $100^\circ\text{W}$ , which correspond to  $\rho_t = 2250 \text{ kg/m}^3$ . Finally, for the third target,

we define the coordinates  $22^\circ\text{N}$ ,  $103^\circ\text{W}$  that corresponds to  $\rho_t = 2750 \text{ kg/m}^3$ , obtaining the following results. Based on the values from the second column of Table I and with  $\rho_t = 1030 \text{ kg/m}^3$ , in the first instance the impact would generate a crater of  $D_{tc} = 9.28 \times 10^4 \text{ m}$ , which would affect 257,158 houses (*i.e.* the number of houses that would be embedded in the crater). Secondly, the radius of the fireball would be  $R_f = 1.36 \times 10^5 \text{ m}$ , affecting 584,240 houses (*i.e.* the number of houses that would be embedded in the fireball radius), according to data from [17]. Finally, the affected area (at least 4 PSI) would be  $S_r = 1.45 \times 10^7 \text{ km}^2$ , which would include all the houses in the Mexican territory. In fact, this affected surface is a million times the surface of our planet.

In relation to the target  $\rho_t = 2250 \text{ kg/m}^3$ , in the first stage, the impact would form a crater with a diameter of  $D_{tc} = 7.15 \times 10^4 \text{ m}$ , which would affect 12,263 houses. Secondly, the radius of the fireball would be  $R_f = 1.36 \times 10^5 \text{ m}$  which would affect 1,764,068 houses.

In the case of the target  $\rho_t = 2750 \text{ kg/m}^3$ , the impact would generate a crater with a diameter of  $D_{tc} = 6.69 \times 10^4 \text{ m}$ , which would affect 39,153 houses. The radius of the fireball would be  $R_f = 1.36 \times 10^5 \text{ m}$ , which would affect 976,454 houses. Finally, the affected area for the case of the targets  $\rho_t = 2250 \text{ kg/m}^3$  and  $\rho_t = 2750 \text{ kg/m}^3$  would be the same as for  $\rho_t = 1030 \text{ kg/m}^3$ . In fact, these three cases share the same value of the radiated energy and magnitude of the earthquake since these values only depend on the mass and velocity of impact.

There are models used to know the possible final mass of a body considering its morphology and composition with a law strength-scaling exponent [14, 15]. Our model assumes that the impactor is spherical and homogeneous and that it impacts with a fraction of the initial mass:  $m_f = (1 - F)m_0$ , where  $m_f$  is the final mass,  $F$  is the percentage of mass loss  $0 < F \leq 0.6$  [19, 44] and  $m_0$  is the initial mass. From these assumptions, it can be seen that  $d_f = (1 - F)^{1/3}d_0$ , where  $d_f$  and  $d_0$  are the final and initial diameters, respectively. In an analogous way, it can be determined for a cylinder  $d_f = (\sqrt{L_f L_i (F - 1)}d_0/L_f)$  where  $L_f$  and  $L_i$  are the final and initial length of the cylinder that surrounds the body, respectively. For this manuscript,  $L_f = d$  in the Eq. (1) to determine the impact velocity and the energy released.

TABLE II. Results obtained by implementing three targets with  $\rho_i = 2750 \text{ kg/m}^3$  and  $F = 0.3$ . The impact velocity is 19.2 km/s, and the energy released is  $2.82 \times 10^{23} \text{ J}$ .

Target density / Parameters	Crater diameter	Crater depth	Fireball radius	Seismic magnitude	Area affected by overpressure
1030 kg/m <sup>3</sup>	$8.91 \times 10^4 \text{ m}$	$3.15 \times 10^4 \text{ m}$			
2250 kg/m <sup>3</sup>	$6.87 \times 10^4 \text{ m}$	$2.43 \times 10^4 \text{ m}$	$1.31 \times 10^5 \text{ m}$	12.4	$1.34 \times 10^7 \text{ km}^2$
2750 kg/m <sup>3</sup>	$6.42 \times 10^4 \text{ m}$	$2.27 \times 10^4 \text{ m}$			

TABLE III. Infrastructural effects caused by the effects of the crater diameter and the fireball radius in comparison with data from [17] and values from Table II.

Target density and geographic situation/ Parameter and infrastructural damage	Houses affected in relation to the crater diameter	Houses affected in relation to the fireball radius
1030 kg/m <sup>3</sup> (21.3°N, 89.5°W)	253, 808	583, 498
2250 kg/m <sup>3</sup> (25°N, 100°W)	10, 344	1, 754, 280
2750 kg/m <sup>3</sup> (22°N, 103°W)	30, 198	922, 398

Based on the above we have recreated the three scenarios for the targets  $\rho_t = 1030 \text{ kg/m}^3$ ,  $\rho_t = 2250 \text{ kg/m}^3$  and  $\rho_t = 2750 \text{ kg/m}^3$  with  $F = 0.3$ , which are typical value for bodies with  $\rho_i = 2750 \text{ kg/m}^3$ , obtaining results of the Table II.

Although the impact velocity is greater than the nominal, the products of this parameter decrease with respect to the scenarios in which  $v_i = 17 \text{ km/s}$  was assumed since the radius of the fireball, the magnitude of the earthquake, and the area affected depend on the energy of the impact. This is diminished by the decrease in the diameter itself.

To contextualize the results of Table II, we again used the website from [17] and created Table III, which shows the number of houses affected in relation to the diameter of the crater and the fireball radius, target density and geographic location. From these data, it can be determined that the largest number of damaged homes would be caused by the fireball radius and would be found at 25°N, 100°W (located approximately 110 km from the city of Monterrey in the state of Nuevo Leon). This same geographical site would have the lowest number of damaged homes, which seems to contrast with what is intuitive. The authors infer that this situation is due to the demographic phenomenon of gentrification that Monterrey presents.

It is a complex task to determine the infrastructure or vulnerability of the population that would be affected by the impact of the body on our planet. Scenarios using extreme values are commonly proposed to calculate the possible effects of this type of event. For instance, [45] used the sigmoid logistic function to fit data related to the physical effects of a body's impact on our planet and population vulnerability, while [46] models the physical effects on the coastal areas limiting impacts to shallow water only.

## 5. Discussion and conclusions

The work presented here provides a useful tool for calculating the impact of an asteroid on Mexican territory and its observational effects. Mexico covers an area of approximately 1,973 million km<sup>2</sup>, which is why studying the interaction and impact of asteroids becomes relevant. From Laboratorio de Ciencias Geoespaciales (LACIGE) from Universidad Nacional Autónoma de México has been making an effort to paying due attention to this phenomenon. These efforts are focused on the development of numerical models like the one presented in this work, as well as the work developed by [47]. We consider that the Eq. (1) for calculate one of the crucial values for the operation of our model, is based on the calculations of [13] and adapted by us to admit any profile of atmospheric density. In addition to this, the equation involves the parameter of the diameter of the body, which can vary depending on the percentage of mass loss because of the drag force that the body experiences.

We have implemented a numerical model that allows us to know the physical effects when an impact of an asteroid occurs over the Mexican territory from initial conditions such as velocity and angle of entry. Additionally, based on data found in the literature (MPI-NASA database), newer parameters were adapted and incorporated for a possible study in the particular context of our study. These parameters are the calculation of the impact velocity, the percentage of the environment seriously affected, the magnitude of the earthquake produced by the impact, and the surface affected by the overpressure; we found that they depended only on the energy released by the impact. All of these parameters were incorporated into the model to calculate the diameter and the crater depth as well as the fireball radius, as presented in the work of [12], but by considering the Mexican geological conditions in a more realistically.

In this work, we also focus on the Chicxulub asteroid impact, which was recreated and studied using existing input data in the literature. For this case, an analysis was performed regarding on the physical and social effects that this impact would cause in our country if a similar event currently occurred, which obtained specific information about the energy released, the radius of the fireball, the diameter and depth of the crater, the magnitude of the earthquake produced, and surface affected by the overpressure. For this same event, we considered an atmospheric density profile modified, which made it possible to calculate a new impact velocity and with it new values for the effects caused by the impact itself.

Two other hypothetical scenarios were modeled by varying the target density for the Chicxulub impact case, namely  $\rho_t = 2, 250$  and  $2,750 \text{ kg/m}^3$ , which corresponds to intermediate and maximum geological densities known over Mexican territory, respectively. To calculate the damage to the infrastructure, we used the [17] website: the tool *information polygons*, which allowed us to know the number of existing houses in a well-defined polygonal region. To create this region, we set a geographic coordinate and input the crater diameter and fireball radius values obtained with our model, generating the desired information. These data allowed to estimating the affected infrastructure close to the impact point. It is important to mention that the model assumes that the impact by the asteroid occurs with a fraction of its initial mass. In addition, our model is a tool that will allow us to make better predictions about the physical phenomena related to the impact of an asteroid in our territory. This model works in a complementary way with [47].

The results obtained from our model are consistent in comparison with other works, such as [12,43]. Table I shows for example that the impact velocity obtained by us differed by 10% or the energy released differed only by 8% with the works before mentioned. Although the model is limited by the average geological density at a depth of 10 meters, it can give us a good approximation for the size of the crater if the object does not exceed an energy released between  $9.4 \times 10^9 - 3.3 \times 10^{10} \text{ J}$  or with a diameter between 0.35 to 0.54 m. In the case of Chicxulub impact, the model provides an upper limits in the values of size of the crater, the affectation that it could produce if this event occurred in other latitudes and longitudes, and even in the depth of the crater, however, it is evident that the number of buildings affected depends on the size of the object and the density of the collision site, but this information is variable over time caused by the dynamics of population growth itself.

In all the scenarios analyzed in this work, the impact velocity obtained by our model is within the accepted limits for this event, which is 13-21 km/s. The model shows that the impact energy released, the values of the diameter and the depth of the crater, as well as the fireball radius, are all consistent with what was reported by [12,34]. We have observed that, for example, the depth of the crater exceeds the values reported by [12]. This difference could be explained if we consider that an important factor in the model is the density

of the target, which in our case is assumed to be that of the site at a depth of 10 m. If a stratification of the target is assumed, however the actual depth may probably be below this value.

Regarding the environmental consequences, our model is consistent with the validity of the data on the magnitude of the earthquake, and radius of the fireball has a maximum range of 1500 km [12, 24, 30]. We use the values of the density for three different targets in order to know the size and depth of the crater that the impact would cause in each of them. As a result of the implementation of this numerical model, it would be possible to predict scenarios of body impacts on our planet, in particular, effects on the environment in the Mexican territory.

In addition, the intense heat generated by the asteroid's entry into the atmosphere can lead to significant heating and expansion of the surrounding air. This heating can cause localized changes in the density and temperature of the ionosphere, see for instance, [48]. Mexico there is also evidence that suggests this can occur. Its break-up and burst have disturbed the intermediate layers of the atmosphere and also the ionosphere. These disturbances have been detected by satellites and probes as unusual behaviors in the total electron content (TEC) and analyzed by [49]. To calculate the effects on the atmosphere produced by the impact of a body with the Earth's surface, the concept of shock wave energy can also be used. The high temperatures and pressures associated with the asteroid impact can cause ionization of the atmospheric gases, leading to the formation of plasma. It is important to mention that the impact of an asteroid can generate electromagnetic pulses (EMPs) that propagate through the atmosphere and ionosphere. All of these effects will be incorporated in a next version of our model.

As an example, the work of [25] determined that the relation between the energy of shock waves and the total energy released is  $E_{sw}/E_i \approx 0.002$ . In the work of [50] proposed that the Chelyabinsk meteoroid released an energy  $E_{sw} = 9.4 \times 10^{12} \text{ J}$ . On the other hand, [51] suggested that the Kamchatka meteoroid released  $E_{sw} = 1.5 \times 10^{12} \text{ J}$ , in both cases these objects caused a low to medium ionospheric disturbance. In the work of [49], the Morelian meteoroid released  $E_i = 5.1 \times 10^{10} \text{ J}$  i.e.,  $E_{sw} = 1.08 \times 10^8 \text{ J}$ , causing a very low ionospheric disturbance. For the Chicxulub event, the energy released in shock waves would be  $E_{sw} = 6.4 \times 10^{20} \text{ J}$ , from which it can be inferred that the ionospheric disturbance would be high.

Finally for our model, the initial values required by this can be adapted and obtained from the final values reported in the work of [47]: these two models works as modules coupled with each other to make a more complete description of the phenomenon in studying the fall of asteroids in the Mexican territory.

## Acknowledgements

The author Gutiérrez-Zalapa wishes to thank the Consejo Nacional de Humanidades Ciencias y Tecnología (CONAH-CyT) for the support in performing this research. He also wishes to thank the Posgrado en Ciencias de la Tierra of the Universidad Nacional Autónoma de México, as well as the Laboratorio de Ciencias Geoespaciales (LACIGE, <https://www.lacige.unam.mx/>) of the Escuela Nacional de Estudios Superiores – Morelia, Michoacán for the facilities provided to perform out the calculations of this paper. M. Rodríguez-Martínez is grateful for the DGAPA PAPIIT/PAPIME projects (IN115423/PE103419) and CONAH-CyT grant INFR:253691. E. Aguilar-Rodríguez is grateful for the DGAPA/PAPIIT project (IN103821).

//www.lacige.unam.mx/) of the Escuela Nacional de Estudios Superiores – Morelia, Michoacán for the facilities provided to perform out the calculations of this paper. M. Rodríguez-Martínez is grateful for the DGAPA PAPIIT/PAPIME projects (IN115423/PE103419) and CONAH-CyT grant INFR:253691. E. Aguilar-Rodríguez is grateful for the DGAPA/PAPIIT project (IN103821).

1. S. Pflanzner *et al.*, The formation of the solar system, *Physica Scripta* **90** (2015) 068001.
2. R. B. Larson, The evolution of molecular clouds, *In The Structure and Content of Molecular Clouds 25 Years of Molecular Radioastronomy*, pp. 13-28 (Springer, 1994).
3. G. W. Wetherill, Formation of the Earth, *Annual Review of Earth and Planetary Sciences* **18** (1990) 205.
4. C. R. Chapman, Impact lethality and risks in today's world: Lessons for interpreting Earth history, *Special Papers- Geological Society Of America* (2002) 7.
5. E. V. Ryan and H. Melosh, Impact fragmentation: From the laboratory to asteroids, *Icarus* **133** (1998) 1.
6. K. R. Housen and K. A. Holsapple, Impact cratering on porous asteroids, *Icarus* **163** (2003) 102.
7. K. Miljković *et al.*, Morphology and population of binary asteroid impact craters, *Earth and Planetary Science Letters* **363** (2013) 121.
8. J. Ormö *et al.*, Boulder exhumation and segregation by impacts on rubble-pile asteroids, *Earth and Planetary Science Letters* **594** (2022) 117713.
9. S. Raducan, T. Davison, and G. Collins, Morphological diversity of impact craters on asteroid (16) Psyche: Insight from numerical models, *Journal of Geophysical Research: Planets* **125** (2020) e2020JE006466.
10. A. Suarez Cortes, A. Flandes, and H. Durand Manterola, Study of Planetary Impact Craters and Their Ejection Material Based on Low Impact Speed Laboratory Models, *LPI Contributions* **2621** (2021) 2031.
11. R. H. Morais *et al.*, Short-Term Consequences of Asteroid Impacts into the Ocean: A Portuguese Case Study, *Universe* **8** (2022) 279.
12. G. S. Collins, H. J. Melosh, and R. A. Marcus, Earth impact effects program: A web-based computer program for calculating the regional environmental consequences of a meteoroid impact on Earth, *Meteoritics & planetary science* **40** (2005) 817.
13. L. T. Elkins-Tanton, Asteroids, meteorites, and comets (Infobase Publishing, 2010).
14. W. Weibull, A statistical distribution function of wide applicability, *Journal of applied mechanics* (1951).
15. V. Svetsov, I. Nemtchinov, and A. Teterov, Disintegration of large meteoroids in Earth's atmosphere: Theoretical models, *Icarus* **116** (1995) 131.
16. L. F. Wheeler *et al.*, Atmospheric energy deposition modeling and inference for varied meteoroid structures, *Icarus* **315** (2018) 79.
17. CENAPRED, Atlas Nacional de Riesgos. Centro Nacional de Prevención de Desastres (2023), <https://www.atlasnacionalderiesgos.gob.mx/>.
18. C. F. Chyba, P. J. Thomas, and K. J. Zahnle, The 1908 Tunguska explosion: atmospheric disruption of a stony asteroid, *Nature* **361** (1993) 40.
19. I. Giblin, New data on the velocity-mass relation in catastrophic disruption, *Planetary and space science* **46** (1998) 921
20. L. Chernogor, Physical effects of the Lipetsk meteoroid: 2, *Kinematics and Physics of Celestial Bodies* **35** (2019) 217.
21. P. Schultz and D. Gault, Seismic effects from major basin formation on the moon and Mercury, *Tech. rep.* (1974).
22. H. J. Melosh, Impact cratering: A geologic process, New York: Oxford University Press; Oxford: Clarendon Press (1989).
23. H. Kanamori and D. L. Anderson, Theoretical basis of some empirical relations in seismology, *Bulletin*.
24. T. C. Hanks and H. Kanamori, A moment magnitude scale, *Journal of Geophysical Research: Solid Earth* **84** (1979) 2348.
25. L. Chernogor, Physical effects of the Lipetsk meteoroid: 3, *Kinematics and Physics of Celestial Bodies* **35** (2019) 271.
26. W. B. Ryan *et al.*, Global multi-resolution topography synthesis, *Geochemistry, Geophysics, Geosystems* **10** (2009).
27. F. D. Stacey and P. M. Davis, Earth, density distribution, *Encyclopedia of Solid Earth Geophysics* (2020) 1.
28. G. H. Stokes *et al.*, Update to determine the feasibility of enhancing the search and characterization of NEOs, Report of the Near-Earth Object Science Definition Team NASA (2017).
29. M. Paine, Environmental damage from asteroid and comet impacts, *The Planetary Society-Australian Volunteer Coordinators* (2004).
30. S. Glasstone *et al.*, The effects of nuclear weapons, **vol. 50** (US Department of Defense, 1977).
31. V. Shuvalov, V. Svetsov, and I. Trubetskaya, An estimate for the size of the area of damage on the Earth's surface after impacts of 10-300-m asteroids, *Solar System Research* **47** (2013) 260.
32. P. Beland, Cretaceous-tertiary extinctions and possible terrestrial and extraterrestrial causes/by the K-TEC group, National Museum of Natural Sciences of Canada (1977).
33. R. Ganapathy, A major meteorite impact on the earth 65 million years ago: Evidence from the Cretaceous-Tertiary boundary clay, *Science* **209** (1980) 921.

34. L. W. Alvarez *et al.*, Extraterrestrial cause for the Cretaceous-Tertiary extinction, *Science* **208** (1980) 1095.
35. L. W. Alvarez, Experimental evidence that an asteroid impact led to the extinction of many species 65 million years ago, *Proceedings of the National Academy of Sciences* **80** (1983) 627.
36. M. Boslough *et al.*, Axial focusing of impact energy in the earth's interior: A possible link to flood basalts and hotspots, Tech. rep., Sandia National Labs., Albuquerque, NM (United States) (1994).
37. M. A. Richards *et al.*, Triggering of the largest Deccan eruptions by the Chicxulub impact, *GSA Bulletin* **127** (2015) 1507.
38. J. Urrutia-Fucugauchi *et al.*, The Chicxulub scientific drilling project (CSDP), *Meteoritics & Planetary Science Archives* **39** (2004) 787.
39. H. J. Durand-Manterola and G. Cordero-Tercero, Assessments of the energy, mass and size of the Chicxulub Impactor, arXiv preprint arXiv:1403.6391 (2014).
40. E. Pierazzo, D. A. Kring, and H. J. Melosh, Hydrocode simulation of the Chicxulub impact event and the production of climatically active gases, *Journal of Geophysical Research: Planets* **103** (1998) 28607.
41. D. A. Kring, The Chicxulub impact event and its environmental consequences at the Cretaceous-Tertiary boundary, Palaeogeography, Palaeoclimatology, *Palaeoecology* **255** (2007) 4.
42. J. Morgan *et al.*, Size and morphology of the Chicxulub impact crater, *Nature* **390** (1997) 472.
43. U. S. N. Oceanic, A. Administration, and U. S. A. Force, U.S. Standard atmosphere, 1976, vol. 76 (National Oceanic and Atmospheric Administration, 1976).
44. Z. Ceplecha and D. O. ReVelle, Fragmentation model of meteoroid motion, mass loss, and radiation in the atmosphere, *Meteoritics & Planetary Science* **40** (2005) 35.
45. C. M. Rumpf, H. G. Lewis, and P. M. Atkinson, Population vulnerability models for asteroid impact risk assessment, *Meteoritics & Planetary Science* **52** (2017) 1082.
46. G. Gisler, R. Weaver, and M. Gittings, Calculations of asteroid impacts into deep and shallow water, *Pure and applied geophysics* **168** (2011) 1187.
47. R. Gutiérrez-Zalapa *et al.*, Modeling the transit of a NEO through the Earth's atmosphere, In *44th COSPAR Scientific Assembly*. **44** (2022) 229.
48. L. Chernogor, Magnetic and ionospheric effects of a meteoroid plume, *Geomagnetism and Aeronomy* **58** (2018) 119.
49. M. A. Sergeeva *et al.*, Assessment of Morelian Meteoroid Impact on Mexican Environment, *Atmosphere* **12** (2021) 185.
50. L. Chernogor, Ionospheric effects of the Chelyabinsk meteoroid, *Geomagnetism and Aeronomy* **55** (2015) 353.
51. Y. Luo and L. Chernogor, Ionospheric Effects of the Kamchatka Meteoroid: Results of GPS Observations, *Kinematics and Physics of Celestial Bodies* **39** (2023) 71.
52. E. A. Silber *et al.*, Physics of meteor generated shock waves in the earth's atmosphere-a review, *Advances in Space Research* **62** (2018) 489.
53. A. Morbidelli *et al.*, Origin and evolution of near-Earth objects, *Asteroids iii* **409** (2002).
54. D. F. Lupishko, M. Di Martino, and R. P. Binzel, Near-Earth objects as principal impactors of the Earth: Physical properties and sources of origin, *Proceedings of the International Astronomical Union* **2** (2006) 251.
55. R. Gutiérrez-Zalapa, Desarrollo de un modelo analítico para el estudio de impactos por asteroides sobre territorio mexicano (2019), Tesis de posgrado. Posgrado en Ciencias de la Tierra. Escuela Nacional de Estudios Superiores unidad Morelia. Universidad Nacional Autónoma de México.
56. INEGI, Población Morelia Michoacán, México (2021), <https://www.inegi.org.mx/app/areasgeograficas/>.
57. D. L. Mathias, L. F. Wheeler, and J. L. Dotson, A probabilistic asteroid impact risk model: assessment of sub-300 m impacts, *Icarus* **289** (2017) 106.
58. L. F. Wheeler, P. J. Register, and D. L. Mathias, A fragment-cloud model for asteroid breakup and atmospheric energy deposition, *Icarus* **295** (2017) 149.
59. I. Nemtchinov *et al.*, Light flashes caused by meteoroid impacts on the lunar surface, *Solar System Research* **32** (1998) 99.
60. H. J. Melosh *et al.*, Remote visual detection of impacts on the lunar surface, In *Lunar and Planetary Science Conference*, **24** (1993).
61. J. Borovicka, The comparison of two methods of determining meteor trajectories from photographs, *Bulletin of the Astronomical Institutes of Czechoslovakia* **41** (1990) 391.
62. S. S. Board, N. R. Council *et al.*, Defending planet earth: Near-Earth-Object surveys and hazard mitigation strategies (National Academies Press, 2010).
63. N. J. Bailey *et al.*, Global vulnerability to near-Earth object impact, *Risk Management* **12** (2010) 31.
64. T. P. Remington *et al.*, Numerical simulations of laboratoryscale, hypervelocity-impact experiments for asteroid-deflection code validation, *Earth and Space Science* **7** (2020) e2018EA000474.
65. J. Deller, Hyper-velocity impacts on rubble pile asteroids (Springer, 2016).
66. P. Mehta, E. Minisci, and M. Vasile, Break-up modelling and trajectory simulation under uncertainty for asteroids, In 4th IAA Planetary Defense Conference, Rome, Italy (2015).
67. J. G. Hills and M. P. Goda, The fragmentation of small asteroids in the atmosphere, *The Astronomical Journal* **105** (1993) 1114.
68. D. Robertson and D. Mathias, Effect of yield curves and porous crush on hydrocode simulations of asteroid airburst, *Journal of Geophysical Research: Planets* **122** (2017) 599.